Catal Lett (2014) 144:809–816
DOI 10.1007/s10562-014-1236-2

Hydrodeoxygenation of Dibenzofuran Over SBA-15 Supported Pt, Pd, and Ru Catalysts

Lei Wang · Chuang Li · Shaohua Jin · Wenzhen Li · Changhai Liang

Received: 5 December 2013 / Accepted: 6 March 2014 / Published online: 21 March 2014

Abstract Hydrodeoxygenation (HDO) of dibenzofuran (DBF) has been carried out over mesoporous silica SBA-15 supported Pt, Pd, and Ru catalysts. The HDO of DBF went through hydrogenation of aromatic rings first, followed by hydrogenolysis of the saturated C–O bond to produce hydrocarbons. The detection of intermediate 2-cyclohexylcyclohexanol over as-prepared Pt catalysts illustrated that the aromatic ring-containing hydrogenated species transformed to the major deoxygenated product bicyclohexane after elimination of the heteroatom oxygen. Among all three catalysts, the Pt/SBA-15 catalysts exhibited the highest hydrogenation activity to yield aromatic ring-containing hydrogenated products. However, the Ru catalysts were more efficient in formation of completely deoxygenated products. Meanwhile, more cleavage of the saturated C–O bond took place at higher reaction temperature in the HDO of DBF. The increase of hydrogen pressure promoted the saturation of aromatic rings with an obvious influence on the conversion of DBF.

Keywords Hydrodeoxygenation · Dibenzofuran · Precious metals · Reaction mechanism

L. Wang · C. Li · S. Jin · C. Liang (✉)
Laboratory of Advanced Materials and Catalytic Engineering, School of Chemical Engineering, Dalian University of Technology, Dalian 116012, China
e-mail: changhai@dlut.edu.cn
URL: http://finechem.dlut.edu.cn/liangchanghai/

W. Li
Department of Chemical Engineering, Michigan Technological University, Houghton, MI, USA

1 Introduction

With the decline of fossil fuel sources, much attention has been focused on developing the next generation of fuels. Renewable energy from biomass transformation is of major interest to reduce the dependence to the fossil fuels [1, 2]. The bio-oils derived from biomass conversion contain high oxygen content, taking up to 40 % in weight, which results in high viscosity, low heating value, and poor thermal stability [3, 4]. Hydrodeoxygenation (HDO) is such a promising process to upgrade the bio-oils to gasoline or diesel for practical use. The conventional HDO catalysts used to hydrotreat oxygen-containing compounds in coal tar or shale oil are NiMo and CoMo sulfides [5–9]. Due to the bio-oils having a tendency for polymerization and less sulfur, these catalysts show some drawbacks in the hydrogenation (HYD) activity and often introduce sulfur into the final products. It is therefore required to develop highly active HDO catalysts that can perform under mild reaction conditions. Precious metal (Pt, Pd, Ru, etc.) catalysts have been demonstrated to show some utilities for aromatics HYD at mild temperature [10–12], and thus are good candidates for HDO of bio-oils.

On the basis of component analysis of the bio-oils, the majority of oxygen-containing compounds are phenols, furans, and ethers [13]. Here, dibenzofuran (DBF) is used as a model compound with furan and aromatic structure to test the activity of HDO catalysts. In the most previous works, HDO of DBF over Ni(Co)Mo sulfide catalysts goes through two routes: the HYD reaction route with aromatic ring HYD occurring, followed by oxygen removal, and the direct deoxygenation (DDO) reaction route through C–O bond hydrogenolysis without ring HYD [7, 8]. Over transition metal sulfide catalysts, the DDO reaction route is favored while less ring HYD is observed [6–8]. Products

obtained from direct hydrogenolysis of the C–O bond of DBF still need further HYD to saturate the aromatic rings before application. Over precious metal catalysts, the HYD reaction route resulting in partially or fully saturated oxygen-containing compounds and deoxygenated hydrocarbons is dominant [14–16]. Although similar product distribution is observed in the hydrotreating process of guaiacol below 250 °C over monometallic catalysts [17, 18], little research focuses on the comparison of HDO product distribution at even higher reaction temperature (i.e. >250 °C). Such studies are desired to give an insight into the HDO product distribution to elucidate the relevant reaction networks. Thus selective HDO was conducted over the monometallic (Pt, Pd, and Ru) catalysts to explore the variation of product distribution influenced by the different kinds of precious metals. The mesoporous support SBA-15 was found to be better than microporous supports in the mass transfer of reactants during reaction [19]. HDO reaction kinetics over Pt, Pd, and Ru supported on SBA-15 catalysts were also investigated with the aim to verify the reaction mechanism and further optimize the HDO product distribution.

2 Experimental

2.1 Catalyst Preparation

SBA-15 was synthesized by using nonionic triblock copolymer P123 as structure-directing agent according to the experimental steps reported before [20]. The supported precious metal catalysts were prepared by the wetness impregnation method with metal precursors $H_2PtCl_6{\cdot}6H_2O$, $Pd(C_2H_3O_2)_2$, and $RuCl_3{\cdot}3H_2O$. Typically, a certain amount of metal precursor was dissolved in 70 mL methanol at room temperature. Then 1.00 g of calcined SBA-15 support was added under vigorous stirring until the formation of homogenous slurry. The slurry was attached to a rotovap, using a bath to maintain the flask at ambient temperature. Methanol was removed after 30 min and the slightly damp powder was allowed to air dry at 60 °C for 6 h prior to reduction. The prepared catalysts were pre-reduced at 400 °C for 2 h under 40 mL/min H_2, having first been heated to the desired temperature from room temperature at a rate of 2 °C/min.

2.2 Catalyst Characterization

X-ray diffraction (XRD) analysis of the samples was carried out using a Rigaku D/Max-RB diffractometer with Cu Kα monochromatized radiation source (λ = 1.54178 Å), operated at 40 kV and 100 mA. Elemental analysis was performed using inductively coupled plasma atomic emission spectroscopy (ICP-AES) (Perkin-Elmer Optima 2000DV). Nitrogen adsorption and desorption isotherms at −196 °C were measured by using a Quadrasorb IQ surface area and pore size analyzer. The specific surface area of SBA-15 support was calculated by Brunauer–Emmett–Teller (BET) method and pore volumes were calculated from the volume of liquid nitrogen at $p/p_0 = 0.99$. Non-local density functional theory (NLDFT) method considering sorption of nitrogen at −196 °C in cylindrical silica pores was used to determine the pore size distribution by using the adsorption branch. TEM images were taken on FEI Tecnai G20. CO chemisorption analysis was performed in a Quadrasorb IQ apparatus under static volumetric conditions. Prior to measurement, the ex situ reduced catalysts were activated in situ in H_2 at 300 °C for 2 h and evacuated for 2 h, then the furnace was cooled to 30 °C. The chemisorption isotherms were obtained by measuring the amount of CO adsorbed for pressures varying from 80 to 560 mmHg at 30 °C. After completing the initial analysis, the reversibly adsorbed gas was evacuated and the analysis repeated to determine the chemisorbed molecules alone. A CO/Metal = 1 stoichiometry was accordingly taken to estimate the number of metal active sites.

2.3 Catalytic Activity Test

Typically, the HDO of DBF experiments were performed at 280 °C and 3.0 MPa total pressure in a continuous-flow fixed-bed reactor over 50 mg catalyst diluted with 5.0 mL 60–80 mesh quartz sands. Before the HDO experiments, the prepared catalysts were activated in situ with 40 mL/min H_2 at 3.0 MPa and 300 °C for 1 h. Then the temperature was adjusted to the reaction temperature. The liquid reactants composed of 3.0 wt% DBF, 1.0 wt% dodecane (as internal standard for gas chromatography (GC) analysis), and 96.0 wt% decane (as inert solvent). The experimental data were collected at different weight time after 14 h until the fresh catalyst reached steady state. The weight time is defined as $\tau = W_{cat}/n_{feed}$, where W_{cat} denotes the catalyst weight and n_{feed} denotes the total molar flow feed to the reactor. The varying of weight time was achieved by changing either the flow rate of liquid reactants or catalyst weight. The reaction products after being condensed in a trap at room temperature were collected and analyzed using an Agilent GC 7890A with a flame ionization detector and a 0.25 μm × 0.32 mm × 30 m HP-5 capillary column. Product identifications were conducted on an Agilent 6890N with 5973 MSD and a 0.25 μm × 0.32 mm × 30 m HP-5MS capillary column. More detailed analysis conditions and reaction data analysis were introduced in a previous publication [21].

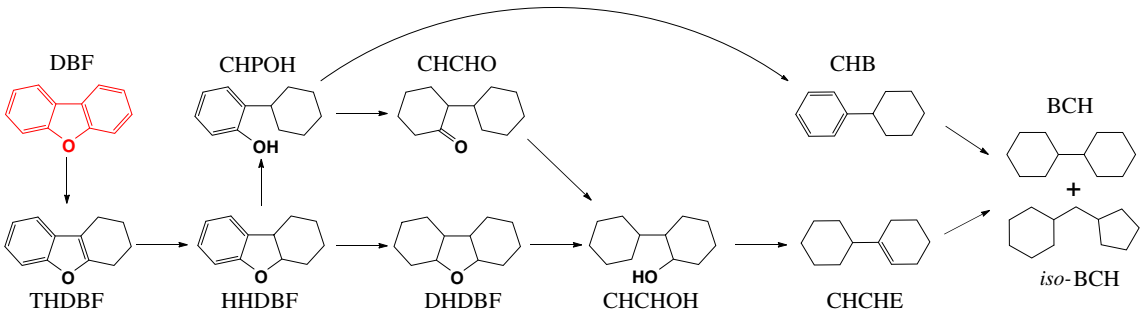

Scheme 1 Proposed reaction network of HDO of DBF over the Pt, Pd, and Ru supported on SBA-15 catalysts

2.4 HDO Reaction Networks

Based on the previous HDO reaction networks of DBF [14, 21, 22], some species detected over the prepared Pt, Pd, Ru/SBA-15 catalysts are shown in Scheme 1. Tetrahydrodibenzofuran (THDBF), hexahydrodibenzofuran (HHDBF), and dodecahydrodibenzofuran (DHDBF) are obtained by partial or total HYD of the aromatic rings of DBF. 2-Cyclohexylphenol (CHPOH), 2-cyclohexylcyclohexanone (CHCHO), and 2-cyclohexylcyclohexanol (CHCHOH) are the oxygen-containing intermediates resulted from C–O cleavage of hydrogenated species or further HYD of CHPOH. Here, the abbreviation OCH is used to represent the sum of CHPOH, CHCHO and CHCHOH products. Unsaturated deoxygenated products, such as cyclohexylbenzene (CHB) and cyclohexenylcyclohexane (CHCHE), are also observed. Bicyclohexane (BCH) and its isomer cyclopentylmethylcyclohexane (*iso*-BCH) are presented in the products. Similarly, the abbreviation CH is defined to represents the sum of CHB, CHCHE, BCH and *iso*-BCH.

3 Results and Discussion

3.1 Catalysts Characterization

The structure of synthesized SBA-15 was confirmed by small-angle XRD as shown in Fig. 1a. Three well-resolved peaks are displayed, which are indexed as (100), (110) and (210) reflections associated with p6mm hexagonal symmetry. This indicates that the prepared SBA-15 contained well-ordered mesoporous structure [23]. The nitrogen adsorption–desorption isotherms of the calcined SBA-15 (Fig. 1b) are classified as type IV isotherms with a clear H1 hysteresis loop. The calcined SBA-15 support contains a BET surface area of 670 m^2/g and a pore volume of 1.20 cm^3/g. It is clear that the pore size calculated from the adsorption branch with the NLDFT method is ~8.0 nm in the insert of Fig. 1b. After loading precious metal, ICP-AES results show that the actual metal loadings of the supported Pt, Pd and Ru/SBA-15 catalysts are 0.97, 0.93, and 0.89 wt%, respectively, which are slight less than the nominal 1.00 wt% metal loading. TEM images of the reduced Pt, Pd, Ru/SBA-15 catalysts are exhibited in Fig. 2. The typical hexagonal structures of SBA-15 are still maintained after loading metal. Metal particles with a narrow particle size distribution are well-distributed on the support and no apparent aggregation is observed.

3.2 HDO Over Pt/SBA-15 Catalysts

Several main products (THDBF, HHDBF, DHDBF, CHCHO, CHCHOH and BCH) in the HDO reaction of DBF over the Pt/SBA-15 were chosen to reveal the overall HDO reaction process. At a high temperature of 280 °C, the HDO of DBF was conducted at low weight time, achieved by reducing the catalyst weight, which was due to the high HYD activity of the Pt/SBA-15 catalysts resulting in almost complete conversion of DBF in the typical reaction conditions. As shown in Fig. 3a, b, partially aromatic ring hydrogenated species THDBF and HHDBF are more prevalent at low weight time (0.15 g min/mol) compared with fully aromatic ring hydrogenated DHDBF, which is attributed to the short contact between reactant DBF and catalysts. With increasing weight time, the amounts of both fully hydrogenated products DHDBF and oxygen-containing saturated intermediates (i.e. CHCHO and CHCHOH) exhibit an increasing trend, reaching a maximum around $\tau = 0.90$ g min/mol. The detected CHCHOH links the oxygen-containing intermediates and totally deoxygenated hydrocarbons in the HDO reaction network of DBF. The deoxygenation reaction route becomes preferred at weight time higher than 0.90 g min/mol. BCH is the main totally deoxygenated product with a product distribution around 30 % at $\tau = 1.07$ g min/mol. Another product DHDBF contributes most of the remaining amount. The HDO product distribution as a function of weight time obviously shows that the whole HDO reaction route goes from HYD of the aromatic rings to deoxygenation of oxygen-containing

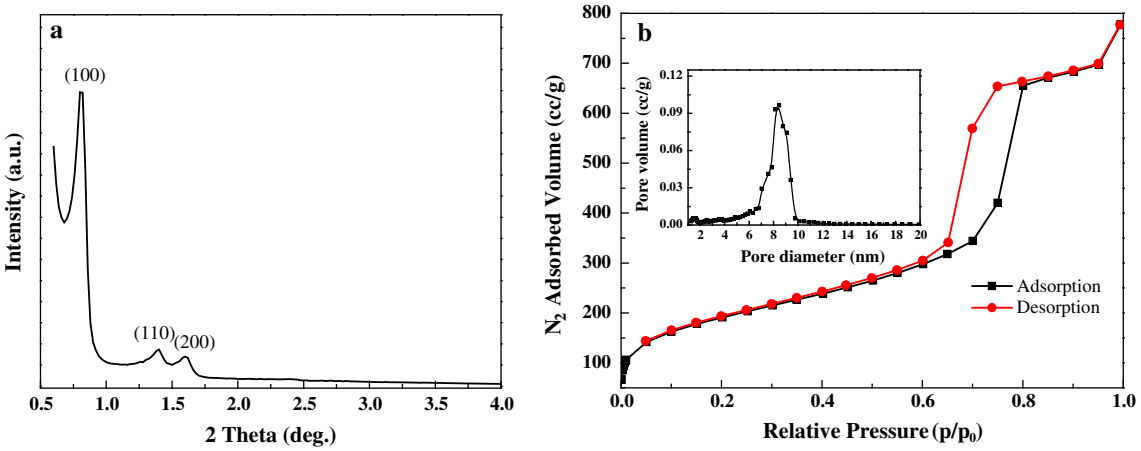

Fig. 1 Small-angle XRD pattern (**a**) and nitrogen adsorption–desorption isotherms (**b**) of the calcined SBA-15 and the insert is the pore size distribution calculated by NLDFT method

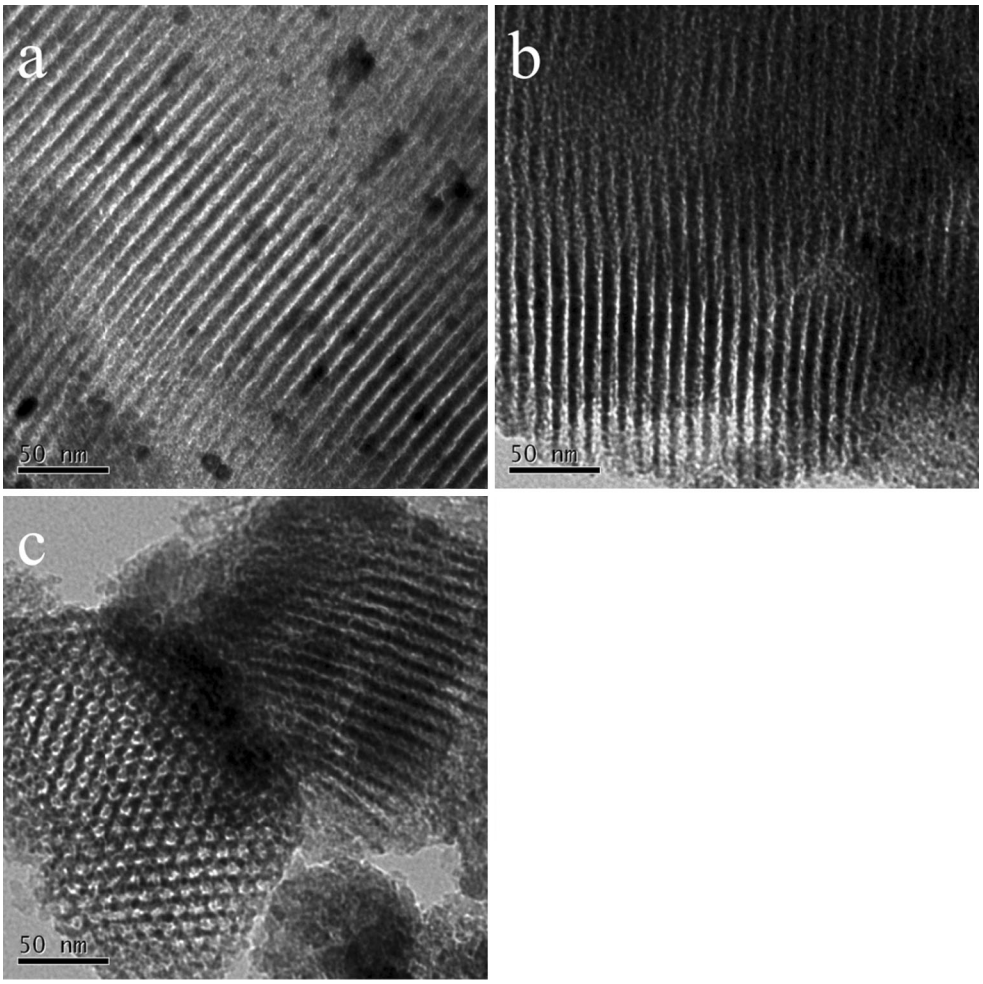

Fig. 2 TEM images of supported Pt/SBA-15 (**a**), Pd/SBA-15 (**b**), and Ru/SBA-15 (**c**) catalysts with 1.00 wt% precious metal loading

intermediates through cleavage of the saturated C–O bond. The detected hydrogenated intermediates help to better understand the HYD sequence of aromatic rings in the DBF molecule.

The HDO of DBF shows a behavior of aromatic ring HYD to THDBF, HHDBF, and DHDBF at low temperature (200 °C), which is similar with previous works about HDO of biomass-derived compounds under mild temperature

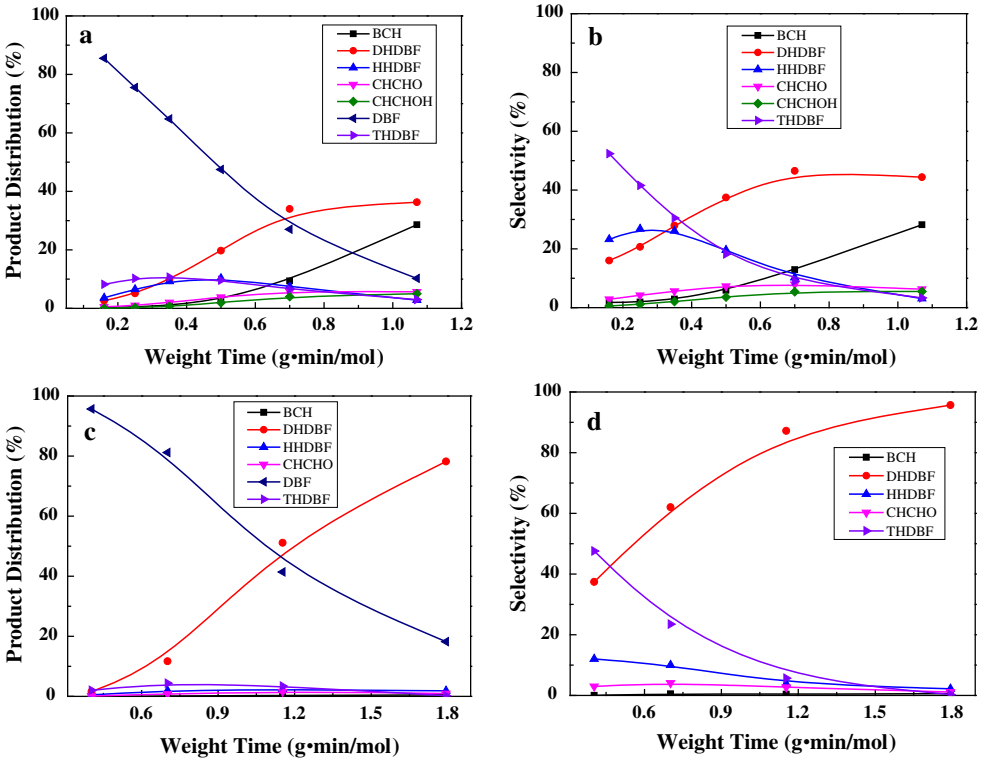

Fig. 3 Product distribution and selectivity of HDO of DBF over Pt/SBA-15 as a function of weight time under 280 °C (**a**, **b**) and 200 °C (**c**, **d**) with 3.0 MPa total pressure

that reported increased aromatic ring hydrogenated products [1]. DHDBF was detected as the main HDO product over the studied weight times from the product distribution in Fig. 3c. At the lowest weight time of $\tau = 0.40$ g min/mol, THDBF and HHDBF were detected, with 48 and 12 % selectivity, respectively (Fig. 3d). From the variations of selectivities toward the hydrogenated DBFs, it is clear that the THDBF and HHDBF undergo further HYD to DHDBF with a high selectivity of 96 % at $\tau = 1.79$ g min/mol.

3.3 HDO of DBF Over Pd/SBA-15 and Ru/SBA-15 Catalysts

The HDO reactions of DBF over the Pd/SBA-15 and Ru/SBA-15 were conducted under similar reaction conditions with varied weight times. Over the Pd/SBA-15 catalysts, the main products THDBF, HHDBF, DHDBF, CHPOH, CHCHO, and BCH are observed (shown in Fig. 4a). CHPOH is preferably obtained from cleavage of the C–O bond linking the saturated aromatic ring and oxygen heteroatom, which is attributed to the higher energy need to break the existing p–π conjugation in benzene ring electrons and oxygen lone-pair electrons [24, 25]. With increasing weight time, almost all the examined products show an increased trend in the HDO products distribution. It is noticeable that the amount of BCH increases from 0 to nearly 18 %. Regarding the variation of selectivity along with the weight time in Fig. 4b, it is clear that the selectivities toward ring hydrogenated species decrease (i.e. 48–10 % for THDBF) and deoxygenated hydrocarbons increase (i.e. 0–24 % for BCH). This varying trend makes an explanation to the change of HDO reaction route from only aromatic ring HYD of DBF to further deoxygenation. A relative abundance of CHPOH with 32 % selectivity at $\tau = 1.15$ g min/mol resulted from insufficient HYD of the phenolic group in the CHPOH to cycloketones and excess cleavage of C–O bond under such high temperature. This leads to reduced selectivity of HHDBF at lower weight times.

Over the Ru/SBA-15 catalysts, many intermediates with small amounts were detected at 280 °C and 3.0 MPa total pressure. HDO product distribution as a function of weight time varies similarly with that over the Pd/SBA-15. A relatively abundant amount (18 %) of deoxygenated product CHB is detected at $\tau = 2.68$ g min/mol, which is quite different from the BCH that make up the highest amount in the captured deoxygenated products over Pt or Pd/SBA-15 catalysts. This phenomenon could be ascribed to the higher hydrogenolysis activity of Ru versus Pt or Pd in the HDO reaction [26]. It provides good evidence that hydrogenolysis of the phenolic hydroxyl group in the CHPOH to CHB without further HYD took place. This is similar with previous findings about direct dehydroxylation of phenols to benzenes [27, 28].

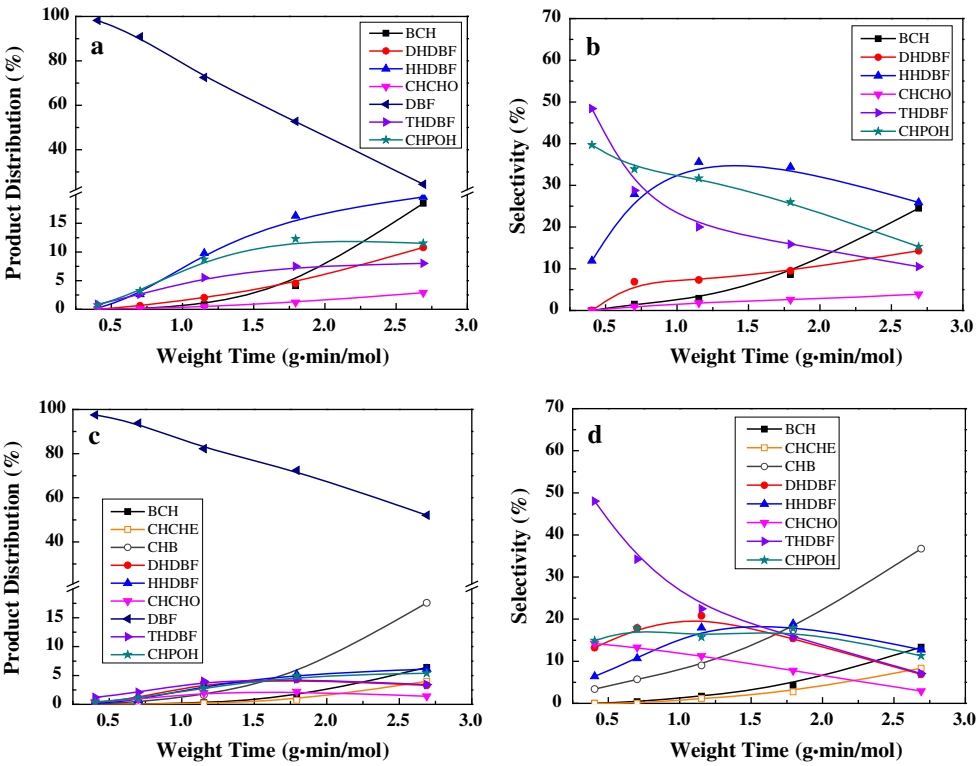

Fig. 4 Product distribution and selectivity of HDO of DBF over Pd/SBA-15 (**a**, **b**) and Ru/SBA-15 (**c**, **d**) as a function of weight time under 280 °C and 3.0 MPa total pressure

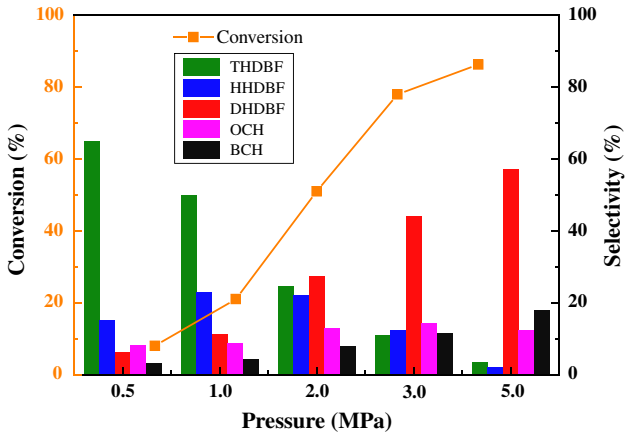

Fig. 5 DBF conversion and product selectivity over Pt/SBA-15 catalysts under 280 °C and $\tau = 0.70$ g min/mol with different total pressures

3.4 Effect of Reaction Pressure

In HYD reactions, the reaction pressure plays a key role on accelerating the rate. Here, the reaction total pressure was varied to give an insight of the influence of hydrogen pressure on the HDO reaction including the conversion of DBF and selectivity of product. In Fig. 5, the HDO conversion increases sharply from 7 to 87 % when the total pressure changes from 0.5 to 5.0 MPa. The selectivities toward DHDBF, BCH, and OCH (the sum of CHPOH, CHCHO, and CHCHOH) simultaneously increase, resulting in better HDO performance via the HYD reaction route. The increased reaction pressure largely promotes the HYD of aromatic rings of DBF to yield more DHDBF, and then C–O bond cleavage is slightly enhanced with up to 18 % selectivity toward BCH. In the sets with low total pressure, it is obvious that THDBF contributes more than 50 % selectivity and the selectivity to HHDBF goes down slightly from 22 to 15 % after adjusting the total pressure from 1.0 to 0.5 MPa.

3.5 Comparative Analysis of HDO Over Pt, Pd, Ru Catalysts

The HDO of DBF over the Pt, Pd, and Ru supported on SBA-15 catalysts apparently proceed through the HYD reaction route, which is quite different from those conducted over the metal sulfide catalysts with both HYD and DDO routes observed. Hydrogenated species with partial or full HYD of aromatic rings in the DBF molecule are detected as shown in Scheme 1. Removal of heteroatom oxygen through saturated C–O bond cleavage is further accomplished, which results in formation of totally deoxygenated products. Turnover frequency (TOF) was calculated according to the CO chemisorption results and HDO conversion to further illustrate the effects of metal on the HDO reaction of DBF. The TOF value calculated at 30 % HDO conversion over the Pt/SBA-15 is 1,196 h^{-1}, which is higher than that over the Pd or Ru catalysts. Although the

Table 1 CO uptakes for the Pt, Pd, and Ru/SBA-15 catalysts and their catalytic activities in the HDO of DBF under 280 °C and 3.0 MPa total pressure

Sample	CO uptake (μmol/g)	TOF (h^{-1})[a]	Initial rates (kPa/(g min))[b]	Selectivity[c]				
				THDBF	HHDBF	DHDBF	OCH	CH
Pt/SBA-15	16.7	1,519	431	35	26	25	11	3
Pd/SBA-15	48.4	13	53	20	35	8	33	4
Ru/SBA-15	13.5	303	34	15	18	15	24	28

[a] Calculated at 30 % HDO conversion

[b] The initial rates was calculated according to the conversion of DBF at the low weight time stages

[c] Selectivity toward THDBF, HHDBF, DHDBF, OCH, and CH at 30 % HDO conversion

Pd/SBA-15 catalyst showed the largest CO uptake (48.4 μmol/g) with more calculated active sites, the lowest TOF with a value of 13 h^{-1} is obtained. At the low weight time stages, HYD of aromatic rings of DBF is the primary reaction in the whole HDO reaction as evidenced by the trends in product distribution as a function of weight times (cf. Figs. 3, 4). By comparing the initial rates, the Pt/SBA-15 contributes the highest value with 431 kPa/(g min) among the prepared supported precious metal catalysts. These HDO reaction results are quite similar with the vapor phase HYD of phenol, which concluded that the supported Pt catalysts are more active than the Pd catalysts [29]. It is interpreted that Pt dissociates molecular hydrogen easily and has a much larger concentration of hydrogen atoms on the metal surface, thus leading to high HYD ability.

The present results conclusively prove that the as-prepared Pt/SBA-15 catalysts are more active than the Pd or Ru catalysts in the HYD of DBF under the studied reaction conditions. In order to further reveal the influence of metal on the DBF transformation, it is desired to compare the selectivities toward HDO products at fixed HDO conversion (i.e. 30 %) under 280 °C and 3.0 MPa total pressure. From Table 1, it is apparent that the Pt catalyst shows high selectivity to hydrogenated DBFs (THDBF, HHDBF, and DHDBF) with a total value of 86 %. Regarding the Pd and Ru catalysts, the saturated C–O bond cleavage is observed with a preference to oxygen containing intermediates (33 %) over Pd catalysts, while the Ru catalysts with strong hydrogenolysis ability selectively transforms the reactant DBF to OCH (24 %) and CH (28 %). From the comparative analysis of the product selectivity, a gradually decreased selectivity to aromatic ring hydrogenated products follows the order Pt > Pd > Ru.

These results also indicate that the prepared Pt/SBA-15 catalyst with better HYD ability selectively promotes the saturation of aromatic rings in the HDO of DBF, thus leading to a high conversion of DBF. Compared with the Pt catalysts, much HHDBF proceeds via C–O bond cleavage to oxygen containing intermediates, which gives rise to a reduced selectivity to DHDBF obtained from further HYD of HHDBF. However, both the Pt and Pd catalysts show limited activity for deoxygenation to yield hydrocarbons (CH) relative to Ru catalysts. In agreement with the above result, Lee et al. [17] found Ru/SiO_2–Al_2O_3 as the best catalysts for HDO of guaiacol in comparison to Pt and Pd. Mortensen et al. [30] concluded Ru was more active catalyst for deoxygenation in the HDO than Pt and Pd. Pt is a catalyst with relatively poor activity for deoxygenation but a very good HYD catalyst. Thus, the present reaction results for HDO of DBF over prepared precious metal catalysts are in good agreement with the literature. The reason that the Ru catalyst has good performance in deoxygenation could be ascribed to the affinity of the metals to bind oxygen. From density functional theory calculations, Nørskov et al. [31] confirmed that Ru has the strongest binding energy with respect to oxygen, and Pt the weakest, which correlates with the affinity for performing deoxygenation.

4 Conclusion

HDO of DBF over mesoporous silica SBA-15 supported precious metal catalysts proceeds through the HYD reaction route, which required a fully saturated benzene ring before the removal of heteroatom oxygen. HDO of DBF yielded more aromatic ring hydrogenated products at 200 °C, while it mainly showed a behavior of deoxygenation of hydrogenated intermediates at the higher temperature of 280 °C. Increasing the hydrogen pressure promoted the conversion of DBF, with selective HYD of THDBF to HHDBF and DHDBF. The Pt/SBA-15 catalysts showed superior HYD activity in the HDO reaction of DBF compared with the Pd and Ru/SBA-15, which resulted in a higher TOF value (1,196 h^{-1}) and initial reaction rate. However, the Ru catalyst was found to be better performing in the deoxygenation of oxygen-containing intermediates to obtain more hydrocarbons. The results show that the right choice of precious metals is required to strike the

appropriate balance between HYD and deoxygenation in the HDO of DBF.

Acknowledgments We gratefully acknowledge the financial support provided by the National Natural Science Foundation of China (21073023), the Fundamental Research Funds for the Central Universities (DUT13RC(3)41), and China Postdoctoral Science Foundation funded project (2013M541220).

References

1. Alonso DM, Wettstein SG, Dumesic JA (2012) Chem Soc Rev 41:8075
2. Corma A, de la Torre O, Renz M, Villandier N (2011) Angew Chem Int Ed 50:2375
3. Choudhary TV, Phillips CB (2011) Appl Catal A 397:1
4. Huber GW, Corma A (2007) Angew Chem Int Ed 46:7184
5. Lavopa V, Satterfield CN (1987) Energy Fuels 1:323
6. Krishnamurthy S, Panvelker S, Shah YT (1981) AlChE J 27:994
7. Girgis MJ, Gates BC (1994) Ind Eng Chem Res 33:1098
8. Girgis MJ, Gates BC (1994) Ind Eng Chem Res 33:2301
9. Romero Y, Richard F, Reneme Y, Brunet S (2009) Appl Catal A 353:46
10. Liu C, Shao Z, Xiao Z, Liang C (2012) React Kinet Mech Catal 107:393
11. Bejblová M, Zámostný P, Červený L, Čejka J (2005) Appl Catal A 296:169
12. Runnebaum RC, Nimmanwudipong T, Limbo RR, Block DE, Gates BC (2012) Catal Lett 142:7
13. Furimsky E (2000) Appl Catal A 199:147
14. Wang YX, Fang YM, He T, Hu HQ, Wu JH (2011) Catal Commun 12:1201
15. Liu C, Shao Z, Xiao Z, Williams CT, Liang C (2012) Energy Fuels 26:4205
16. Zhao C, Kou Y, Lemonidou AA, Li XB, Lercher JA (2009) Angew Chem Int Ed 48:3987
17. Lee CR, Yoon JS, Suh YW, Choi JW, Ha JM, Suh DJ, Park YK (2012) Catal Commun 17:54
18. Bui VN, Laurenti D, Delichère P, Geantet C (2011) Appl Catal B 101:246
19. Stocker M (2008) Angew Chem Int Ed 47:9200
20. Zhao DY, Feng JL, Huo QS, Melosh N, Fredrickson GH, Chmelka BF, Stucky GD (1998) Science 279:548
21. Wang L, Zhang M, Zhang M, Sha G, Liang C (2013) Energy Fuels 27:2209
22. Cecilia JA, Infantes-Molina A, Rodriguez-Castellon E, Jimenez-Lopez A, Oyama ST (2013) Appl Catal B 136:140
23. Kruk M, Jaroniec M, Ko CH, Ryoo R (2000) Chem Mater 12:1961
24. Resasco DE (2011) J Phys Chem Lett 2:2294
25. Hicks JC (2011) J Phys Chem Lett 2:2280
26. Shabtai J, Nag NK, Massoth FE (1987) J Catal 104:413
27. Zhu XL, Lobban LL, Mallinson RG, Resasco DE (2011) J Catal 281:21
28. Zhao C, Kou Y, Lemonidou AA, Li XB, Lercher JA (2010) Chem Commun 46:412
29. Talukdar AK, Bhattacharyya KG, Sivasanker S (1993) Appl Catal A 96:229
30. Mortensen PM, Grunwaldt JD, Jensen PA, Jensen AD (2013) ACS Catal 3:1774
31. Nørskov JK, Rossmeisl J, Logadottir A, Lindqvist L, Kitchin JR, Bligaard T, Jonsson H (2004) J Phys Chem B 108:17886